Influence of Asn/His L166 on the Hydrogen-Bonding Pattern and Redox Potential of the Primary Donor of Purple Bacterial Reaction Centers†

Anabella Ivancich‡ and Tony A. Mattioli*

Section de Biophysique des Protéines et des Membranes, Département de Biologie Cellulaire et Moléculaire, CEA and CNRS URA 2096, CEA/Saclay, 91191 Gif-sur-Yvette Cedex, France

Katie Artz, Shaojie Wang, James P. Allen, and JoAnn C. Williams

Department of Chemistry and Biochemistry and Center for the Study of Early Events in Photosynthesis, Box 871604, Arizona State University, Tempe, Arizona 85287-1604

Received October 8, 1996; Revised Manuscript Received January 13, 1997⊗

ABSTRACT: The primary electron donor (P) of the photosynthetic reaction center (RC) from the purple bacterium *Rhodobacter* (*Rb.*) *sphaeroides* is constituted of two bacteriochlorophyll molecules in excitonic interaction. The C_2 acetyl carbonyl group of one of the two bacteriochlorophyll molecules (P_L), the one more closely associated with the L polypeptide subunit, is engaged in a hydrogen bond with histidine L168, while the other π-conjugated carbonyl groups of P are free from such hydrogen-bonding interactions. The three-dimensional X-ray crystal structures of the RC from several strains of *Rb. sphaeroides* reveal that asparagine L166 probably interacts indirectly with P through His L168. Such an interaction is expected to modulate the hydrogen bond between P and His L168, a residue which is highly conserved in purple bacteria. RC mutants of *Rb. sphaeroides* where asparagine L166 was genetically replaced by leucine [NL(L166)], histidine [NH(L166)], and aspartate [ND(L166)] were studied using Fourier transform (FT) Raman spectroscopy. All of these mutations resulted in an increase in the strength of the hydrogen bond between His L168 and the acetyl carbonyl group of P_L, as observed in the FT Raman spectrum, by the 2−4 cm^{-1} decrease in vibrational frequency of the 1620 cm^{-1} band which has been assigned to this specific acetyl carbonyl group [Mattioli, T. A., Lin, X., Allen, J. P., & Williams, J. C. (1995) *Biochemistry 34*, 6142−6152]. At pH 8, the NH(L166) mutation showed the greatest change in the $P^0/P^{\bullet+}$ redox midpoint potential (515 mV), increasing it by ca. 30 mV compared to that of wild type (485 mV). A similar increase in $P^0/P^{\bullet+}$ redox midpoint potential for NH(L166) compared to that of wild type is also observed at pH 5, 6, and 9.5. The $P^0/P^{\bullet+}$ midpoint potential of the NL(L166) mutant was comparable to that of wild type at all pH values. In contrast, for the ND(L166) mutant, the midpoint potential shows a markedly different pH dependency, being 25 mV higher than wild type at pH 5 but 20 mV lower than wild type at pH 9.5. The hydrogen bond interactions of the primary electron donor from *Rhodospirillum* (*Rsp.*) *centenum* were determined from the FT Raman vibrational spectrum which exhibits a 1616 cm^{-1} band similar to what is seen in the NH(L166) and ND(L166) *Rb. sphaeroides* mutants. Comparison of the sequence of the L subunit determined for the *Rsp. centenum* RC with that of other species indicates that positions L166 and L168 are occupied by His residues. The stronger hydrogen bond between the conserved His L168 and the acetyl carbonyl group of P_L, observed in the primary donor of *Rsp. centenum* and of several bacterial species which are known to possess a histidine residue at the analogous L166 position, is proposed to be due to interactions between these two histidine residues.

The photosynthetic bacterial reaction center (RC)[1] is an integral membrane protein−pigment complex mediating the primary light reactions and subsequent transmembrane charge separation. To date, the three-dimensional X-ray crystal structures of RCs from two species of photosynthetic purple bacteria, *Rhodopseudomonas* (*Rps.*) *viridis* and *Rhodobacter* (*Rb.*) *sphaeroides*, are known (Michel *et al.*, 1986; Allen *et al.*, 1987), both exhibiting a similar general "architecture". The crystal structure of the RC from *Rb. sphaeroides* (Yeates *et al*., 1988; El-Kabbani *et al*., 1991; Chirino *et al*., 1994; Ermler *et al*., 1994; Arnoux & Reiss-Husson, 1996) reveals that the arrangement of the pigment cofactors is associated with the so-called L and M core polypeptides. These cofactors include a dimer of excitonically coupled bacteriochlorophyll *a* (BChl *a*) molecules, designated P_L and P_M, constituting the primary electron donor (P), two accessory monomeric BChl *a* molecules, two bacteriopheophytin *a* molecules, two (ubi)quinones, a non-heme iron atom, and a carotenoid molecule. The RC from *Rps. viridis* (Deisenhofer & Michel, 1989; Deisenhofer *et al*., 1995) contains an

† This work was supported by NIH Grant GM45902 to J.C.W. A.I. gratefully acknowledges a fellowship from CONICET (Argentina).

* Corresponding author.

‡ Present address: DRFMC/SCIB, CEA/Grenoble, 17 rue des Martyrs, 38054 Grenoble Cedex, France.

⊗ Abstract published in *Advance ACS Abstracts,* February 15, 1997.

[1] Abbreviations: *C., Chromatium*; CAPS, 3-(cyclohexylamino)-1-propanesulfonic acid; CHES, 2-(*n*-cyclohexylamino)ethanesulfonic acid; EDTA, ethylenediaminetetraacetic acid; FWHM, full width at half-maximum; HOMO, highest occupied molecular orbital; LDAO, lauryl dimethylamine oxide; MES, 2-(*N*-morpholino)ethanesulfonic acid; RC, reaction center; *Rb*., *Rhodobacter*; *Rps*., *Rhodopseudomonas*; *Rsp*., *Rhodospirillum*; *Rvx*., *Rubrivivax*; Tris, tris(hydroxymethyl)aminomethane.

S0006-2960(96)02516-0 CCC: $14.00

additional protein subunit, a tightly bound tetraheme cytochrome *c*. RC-associated tetraheme cytochromes are also present in many other purple bacteria [reviewed in Nitschke and Dracheva (1995)].

The primary electron donor is a crucial redox component in the RC. In particular, the oxidation potential of P is an important property in the electron-transfer reactions involving P as it, in part, defines the driving force of these reactions [see review by Allen and Williams (1995)]. It has been recently shown that the addition of H-bonds, donated by histidinyl residues, to the conjugated carbonyl groups of P in *Rb. sphaeroides* RCs, systematically raises the $P^0/P^{\bullet+}$ redox midpoint potential from 410 mV (case of no H-bonds) to 765 mV (case of four H-bonds) (Lin *et al.*, 1994a; Mattioli *et al.*, 1995). This mechanism appears to be operational in other native RCs such as that of *Chloroflexus aurantiacus* where the absence of any H-bond donated by a histidinyl residue was proposed to be primarily responsible for the ca. 100 mV lower $P^0/P^{\bullet+}$ redox midpoint potential of this latter species as compared to *Rb. sphaeroides* (Ivancich *et al.*, 1996a).

The three-dimensional crystal structure of the *Rb. sphaeroides* RC shows that the hydrogen-bonding pattern of the π-conjugated carbonyl groups of the primary donor is asymmetric and that only one conjugated carbonyl of P (that of the C_2 acetyl carbonyl of P_L) is H-bonded, the donor being His L168, a residue that is strongly conserved in most purple bacteria (Komiya *et al.*, 1988; Nagashima *et al.*, 1994). This H-bond pattern is entirely consistent with the near-infrared Fourier transform (FT) (pre)resonance Raman spectrum of P in *Rb. sphaeroides* RCs (Mattioli *et al*., 1991, 1994). The vibrational frequency for this H-bonded C_2 acetyl carbonyl group of P_L was observed at 1620 cm^{-1} (Mattioli *et al*., 1991, 1994), indicative of a strong H-bond. The FT Raman spectra of the primary donors from RCs of *Rb. capsulatus* and *Rhodospirillum (Rsp.) rubrum* (Mattioli *et al*., 1992), whose three-dimensional structures are not yet known, also exhibited a FT Raman band at ca. 1620 cm^{-1}, similar to that observed for *Rb. sphaeroides*. The conservation of the histidine L168 residue of *Rb. sphaeroides* in the primary structures of *Rb. capsulatus* and *Rsp. rubrum* (Komiya *et al*., 1988), and assuming a structural analogy of these three RCs, permitted the assignment of the 1620 cm^{-1} band as arising from a similarly H-bonded P_L C_2 acetyl carbonyl group of these primary donors (Mattioli *et al*., 1992).

Interestingly, in the FT Raman spectrum of P from *Rubrivivax* (formerly *Rhodocyclus*) *gelatinosus* RCs, the corresponding band attributable to the P_L C_2 acetyl carbonyl vibrational frequency was reported to be at 1616 cm^{-1} (Agalidis *et al.*, 1992) and not 1620 cm^{-1} as is the case for *Rb. sphaeroides*; this frequency still indicated that the P_L acetyl carbonyl group was engaged in a H-bond but the 4 cm^{-1} lower vibrational frequency, relative to that of *Rb. sphaeroides*, reflected a stronger H-bond. The proposed sequence alignment of the L subunit of *Rvx. gelatinosus* (Nagashima *et al.*, 1993, 1994) with those of *Rb. sphaeroides*, *Rb. capsulatus*, and *Rsp. rubrum* reveals that His L168 is also conserved in *Rvx. gelatinosus*. Very recently, a similar 1616 cm^{-1} band was observed in the FT Raman spectrum of P in RCs of *Chromatium* (*C.*) *tepidum* (Ivancich *et al*., 1996b) which also possess a His residue at the analogous L168 position in *Rb. sphaeroides* (Nozawa *et al.*, 1997). This band was also assigned to the C_2 acetyl carbonyl group of P_L engaged in a H-bond, stronger than that observed in *Rb. sphaeroides*, donated by the same conserved histidinyl residue. In this paper we address the questions: what common structural feature in the RCs of *Rvx. gelatinosus* and *C. tepidum* strengthens the H-bond between the C_2 acetyl carbonyl group of P_L and this highly conserved histidine residue, and does this modest strengthening affect the $P^0/P^{\bullet+}$ redox midpoint potential?

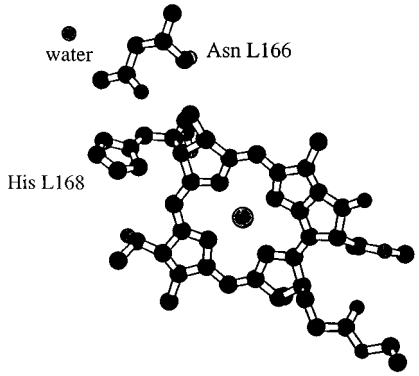

FIGURE 1: View of one of the two bacteriochlorophyll molecules (P_L) constituting the primary electron donor of *Rb. sphaeroides* and the amino acid residues Asn L166 and His L168. His L168 is hydrogen bonded to the acetyl carbonyl of P_L, and Asn L166 is within hydrogen-bonding distance to His L168. In the model of Ermler *et al.* (1994), Asn L166 is within hydrogen-bonding distance to the water molecule shown. Asn L166 is also near Asp M184 (not shown). The view is with the C_2 symmetry axis approximately in the plane of the figure with the periplasmic side at the top. The phytyl chain of the bacteriochlorophyll has been truncated for clarity.

Position L166 in *Rb. sphaeroides*, *Rb. capsulatus*, and *Rsp. rubrum* is occupied by an asparagine residue; in *Rvx. gelatinosus* (Nagashima *et al.*, 1993, 1994) and *C. tepidum* (Nozawa *et al.*, 1996, Ivancich *et al*., 1996b) a histidine is present. According to the RC crystal structures of several strains of the *Rb. sphaeroides* (Yeates *et al.*, 1988, El-Kabbani *et al.*, 1991; Chirino *et al.*, 1994; Ermler *et al.*, 1994, Arnoux & Reiss-Husson, 1996), both the NH_2 group and the carbonyl group of Asn L166 are within hydrogen-bonding distance of His L168 (see Figure 1). The type of amino acid at L166 should influence the strength of the H-bond between His L168 and the primary donor.

In order to test whether the stronger H-bond on the acetyl carbonyl of the primary donors of *Rvx. gelatinosus* and *C. tepidum* compared to those of *Rb. sphaeroides*, *Rb. capsulatus*, and *Rsp. rubrum* is actually due to the presence of histidine instead of asparagine at the analogous position of L166, we have designed a model system consisting of a series of mutant RCs of *Rb. sphaeroides* at position L166. As well, this model system permits us to study the possible effects of this strengthened H-bond on the $P^0/P^{\bullet+}$ redox midpoint potential of the primary electron donor. As a further example, we have determined the H-bond interactions of the primary donor of reaction centers from *Rsp. centenum*.

Rsp. centenum is a purple non-sulfur bacterium of the Rhodospirillaceae family that belongs to the same genus as *Rsp. rubrum* and *Rsp. molischianum*, although it has been recently proposed to be transferred to a new genus, as *Rhodocista centenaria* (Kawaski *et al*., 1992). On the basis of the 16S rRNA classification (Woese, 1987) *Rsp. centenum* is grouped in the α-subclass of Proteobacteria (Imhoff, 1995; Weckesser, 1995). Like *Rps. viridis* and *Rb. sphaeroides*,

the RC is constituted of the homologous L, M, and H polypeptide subunits with apparent molecular masses of 25, 27, and 31 kDa, respectively, and, like *Rb. sphaeroides*, binds *a*-type bacteriochlorin pigments with a BChl:BPhe ratio of 4:2 (Yildiz *et al.*, 1992a). The room temperature electronic absorption spectrum of *Rsp. centenum* RCs exhibits three characteristic bands of other purple bacterial RCs (Yildiz *et al*., 1992a), at 776, 800, and 850 nm arising from the BPhe molecules, the monomeric BChl molecules, and the primary electron donor, respectively. The oxidized RC spectrum exhibits a $P^{\bullet+}$ absorption band at ca. 1242 nm, similar to that of *Rb. sphaeroides* (Wang *et al.*, 1994). The RCs from *Rsp. centenum* possess an associated tetraheme cytochrome *c* subunit, which is not tightly bound as in the case of *Rps. viridis* but can be detached from the RC (Yildiz *et al*., 1992a) as in the case of *C. vinosum* (Romijn & Amesz, 1977) and *C. tepidum* (Nozawa *et al*., 1987). The $P^0/P^{\bullet+}$ redox midpoint potential was measured to be +475 mV in isolated RCs from *Rsp. centenum* containing the tetraheme cytochrome subunit (Wang *et al.*, 1994), a value similar to that of *Rb. sphaeroides* (Lin *et al*., 1994a). In this work, we have determined the H-bonding pattern and the protein interactions of the primary electron donor of the *Rsp. centenum* RC by using near-infrared FT (pre)resonance Raman spectroscopy (Mattioli *et al*., 1991, 1992). From the amino acid residues deduced from the sequence of the gene encoding the *Rsp. centenum* L subunit compared with that of *Rb. sphaeroides*, we propose residues responsible for the observed P H-bonding pattern.

MATERIALS AND METHODS

Mutagensis and DNA Sequencing. *Rb. sphaeroides* reaction center mutants were constructed by oligonucleotide-directed mutagenesis as described by Barik (1993) using thermostable DNA polymerase (New England Biolabs). The vectors containing the L and M subunit genes have been described elsewhere (Lin *et al*., 1994b). The genes were expressed in the *Rb. sphaeroides* deletion strain ΔLM1.1 (Paddock *et al.*, 1989). The wild-type RCs were those isolated from the deletion strain complemented with a plasmid bearing the wild-type genes.

The region of DNA from *Rsp. centenum* containing the *puf* operon, which encodes the L and M subunits of the reaction center, has been previously identified on a genomic insert of the cosmid pFY7 (Yildiz *et al.*, 1992b). The location of the L subunit gene on this cosmid was determined by hybridization with DNA that contains the L and M subunit genes of *Rb. sphaeroides*. The restriction fragments that hybridized with the probe were cloned into M13mp18 and mp19 (Yanisch-Perron *et al.*, 1985) and sequenced by the dideoxy chain-termination method (Sanger *et al.*, 1977) using modified T7 DNA polymerase (United States Biochemicals).

Bacterial Growth and Reaction Center Isolation. The *Rb. sphaeroides* mutants were grown under nonphotosynthetic conditions, and the RCs were isolated using procedures described previously (Williams *et al.*, 1992). Cultures of *Rsp. centenum* were grown, and RCs possessing a bound RC-associated tetraheme cytochrome were isolated as described elsewhere (Wang *et al.*, 1994). Final RC proteins were in 15 mM Tris-HCl, pH 8, 0.025% LDAO, and 1 mM EDTA.

Absorption Spectroscopy. Absorption spectra of isolated RCs were measured at room temperature and at ca. 80 K using a Cary 5 spectrophotometer. For low-temperature measurements, RCs were mixed with glycerol added to a final concentration of 67% (v/v). Samples were measured at ca. 80 K using a 0.15 cm path-length sample holder with quartz windows mounted to a cold tip immersed in liquid nitrogen.

Chemical Redox Titrations. The $P^0/P^{\bullet+}$ redox midpoint potentials were determined by chemical redox titrations using ferricyanide and sodium ascorbate as described elsewhere (Williams *et al*., 1992). For the redox titrations the RCs were resuspended in 100 mM sodium acetate, 100 mM MES, 100 mM Tris, or 100 mM CHES, all with 0.05% Triton X-100 and 1 mM EDTA for pH 5, 6, 8, and 9.5, respectively.

The extent of P reduction was monitored by the absorbance of the P Q_y absorption band (ca. 865 nm) at different ambient potentials. The relative amount of reduced P as a function of ambient potential was fit according to the $n = 1$ Nernst equation. The absorbance of the fully oxidized $P^{\bullet+}$ state was measured by light bleaching. Errors were estimated at better than ±10 mV.

Fourier Transform (FT) Raman Spectroscopy. Room temperature FT (pre)resonance Raman spectra were recorded using a Bruker IFS 66 interferometer coupled to a Bruker FRA 106 Raman module equipped with a continuous, diode-pumped Nd:YAG laser (Mattioli *et al*., 1991). RC samples were contained in a sapphire cell and excited with 180 mW of 1064 nm laser radiation. Spectral resolution was at 4 cm^{-1}. RC samples were in 15 mM Tris-HCl, pH 8.0, 1 mM EDTA, and 0.025% LDAO. For the pH dependence measurements, RC samples were resuspended in 50 mM CAPS (pH = 10.5), or 50 mM Tris-HCl (pH = 8.0), or 50 mM sodium acetate (pH = 5.0), all in 0.05% Triton X-100. For the FT Raman experiments, RC samples were treated with sodium ascorbate and potassium ferricyanide to poise them in their reduced (P^0) and oxidized ($P^{\bullet+}$) states, respectively.

RESULTS

NL(L166), NH(L166), and ND(L166) Mutations in Rb. sphaeroides RCs. The NL(L166), NH(L166), and ND(L166) RC mutants all showed electronic absorption spectra at room temperature which were comparable to that of wild type (WT) (data not shown). At 80 K, spectral differences are observed in the peak position of the Q_y absorption band of the dimer with positions at 884, 875, and 880 nm for NL-(L166), NH(L166), and ND(L166), respectively, compared to 891 nm for WT (Figure 2). Figure 3 shows the room temperature FT Raman spectra, in the 1600−1800 cm^{-1} spectral region, of the *Rb. sphaeroides* L166 mutant RCs compared to that of wild type, all in their reduced P^0 states. The assignments of the bands arising from the two C_2 acetyl and two C_9 keto carbonyl groups of the primary donor dimer of *Rb. sphaeroides* are reported elsewhere (Mattioli *et al.*, 1991, 1994). The FT Raman spectra for the NL(L166), NH-(L166), and ND(L166) mutant RCs do not show drastic changes in the carbonyl vibrational frequencies, indicating that no new H-bonds have been formed on the primary donor of the mutant *Rb. sphaeroides* RCs nor has the existing one on the P_L C_2 acetyl carbonyl been broken. In particular, the C_2 acetyl and C_9 keto carbonyl groups of P_M in this series of mutants exhibit the same vibrational frequencies as those of WT *Rb. sphaeroides* RCs (1653 and 1679 cm^{-1}, respec-

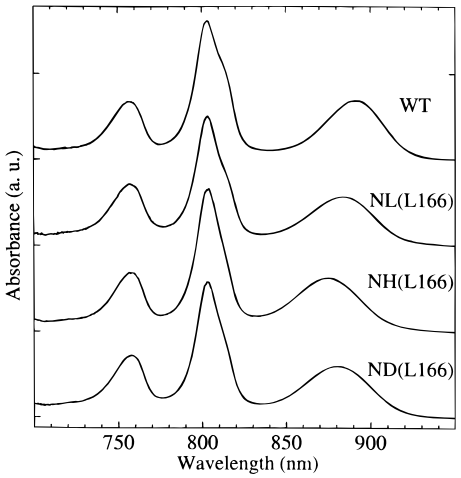

FIGURE 2: Low-temperature (80 K) optical absorption spectra of reaction centers isolated from wild type (WT) and the L166 mutants. The Q_y absorption band centered at 891 nm in WT is slightly shifted to 884, 875, and 880 nm in NL(L166), NH(L166), and ND(L166), respectively. The spectra are normalized at 760 nm.

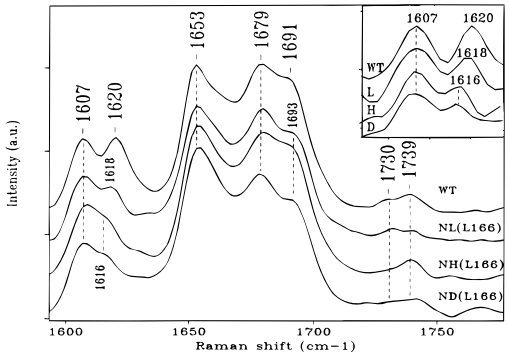

FIGURE 3: Fourier transform Raman spectra in the 1600−1750 cm^{-1} region of reaction centers of *Rb. sphaeroides* wild type (WT) and its NL(L166), NH(L166), and ND(L166) mutants, all poised in their reduced P^0 state with the addition of ascorbate, pH 8. The inset shows the Fourier deconvolution of the 1600−1620 cm^{-1} spectral region. Conditions: room temperature, 1064 nm excitation, 180 mW, coaddition of 4000 scans, and spectral resolution 4 cm^{-1}.

tively). However, the vibrational frequencies of both the C_2 acetyl and the C_9 keto carbonyl groups of P_L are modestly affected by the mutations.

The FT Raman band assigned to the P_L C_2 acetyl carbonyl group (1620 cm^{-1} in WT) appears to decrease in vibrational frequency to 1618 cm^{-1} in the NL(L166) mutant spectrum and to 1616 cm^{-1} in the NH(L166) and ND(L166) mutant spectra; as well, the relative intensities of the 1618−1616 cm^{-1} band as compared to the 1607 cm^{-1} band in each spectrum are lower for the three mutants than for wild type (see Figure 3 and inset). The peak maxima for these latter bands were determined by Fourier deconvolution and second derivative analyses. These two different methods of analysis yielded the same values, and we estimate the error to be ca. ±1 cm^{-1}. The inset in Figure 3 exhibits the Fourier deconvolved spectra in the frequency range of ca. 1600−1630 cm^{-1}. In the three mutant spectra, the 2 or 4 cm^{-1} downshift of the band assigned to the H-bonded C_2 acetyl carbonyl group is clearly observed and indicates a strengthening of this H-bond donated by His L168. The vibrational frequency assigned to the P_L C_9 keto carbonyl group in WT (1691 cm^{-1}) upshifts 3 cm^{-1} for the three mutants (see Figure 3). We have noted in other *Rb. sphaeroides* RC mutants

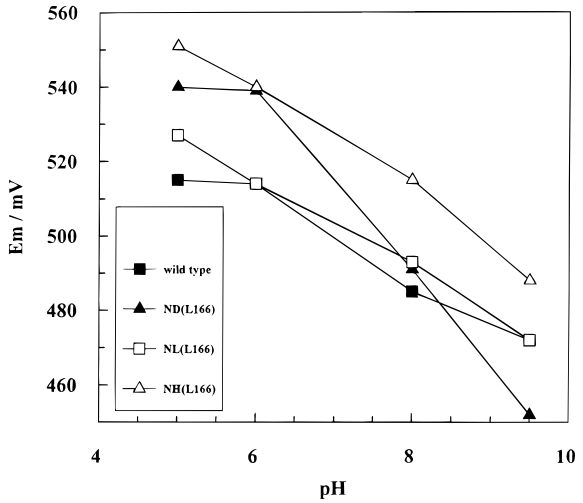

FIGURE 4: Observed variation of the $P^0/P^{\bullet+}$ redox midpoint potential (E_m) of reaction centers of *Rb. sphaeroides* wild type (WT) and its NL(L166), NH(L166), and ND(L166) mutants as a function of pH.

Table 1: $P^0/P^{\bullet+}$ Redox Midpoint Potentials of Wild Type and the L166 Mutants at Various pH Values

residue at L166	E_m (mV) pH 5	E_m (mV) pH 6	E_m (mV) pH 8	E_m (mV) pH 9.5	ΔE_m/pH (mV/pH)[a]
N (wild type)	515	514	485	472	−12
D	540	539	491	452	−25
L	527	514	493	472	−19
H	551	540	515	488	−15

[a] Calculated average change in E_m over the pH range 6−9.5.

that the 1691 cm^{-1} may upshift by 4−5 cm^{-1} as a secondary effect caused by the shift on the 1620 cm^{-1} band (Mattioli *et al*., 1994, 1995). The series of mutations presented here clearly demonstrates that the strength of the H-bond on the C_2 acetyl carbonyl of P_L, donated by His L168, can be increased by changing the amino acid residue at position L166.

pH Dependence Studies. Results of the chemical redox titrations at various pH values for the *Rb. sphaeroides* mutant RCs are shown in Figure 4 and summarized in Table 1. At pH 8, only the NH(L166) mutation appears to significantly modify the $P^0/P^{\bullet+}$ redox midpoint potential, raising it +30 mV as compared to WT. The $P^0/P^{\bullet+}$ midpoint potential of WT RCs exhibits a modest pH dependency, similar to that reported by Maroti and Wraight (1988). In general, as the pH is increased, the $P^0/P^{\bullet+}$ midpoint potentials for WT and the NL(L166), NH(L166), and ND(L166) mutants all decrease. This behavior is consistent with the change in protonation state of many RC residues with different pK_a values (Maroti & Wraight, 1988). The $P^0/P^{\bullet+}$ midpoint potential of the NL(L166) mutant showed a pH dependency very similar to that of WT; as the pH was raised from 5 to 9.5, the $P^0/P^{\bullet+}$ midpoint potential decreased by 55 mV. For the NH(L166) mutant the $P^0/P^{\bullet+}$ midpoint potential decreased 63 mV as the pH was raised from 5 to 9.5 and remained consistently higher by +36 to +16 mV than that for WT for all pH values measured. The most pronounced pH dependence was observed for the ND(L166) mutant with the midpoint potential decreasing by 88 mV as the pH is raised from 5 to 9.5. In Figure 4, the slope of the ND(L166) mutant in the pH range 6−8 is roughly twice that of WT and those of NL(L166) and NH(L166). This greater dependence on pH only observed for the Asp L166 mutant strongly suggests

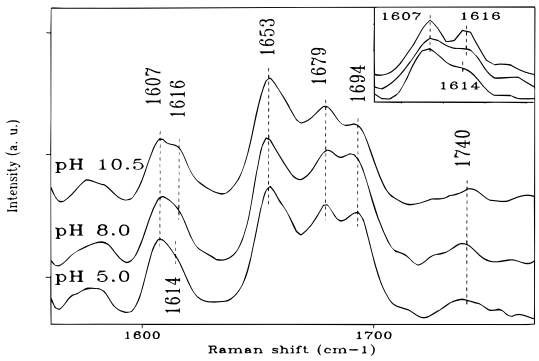

FIGURE 5: Fourier transform Raman spectra of the *Rb. sphaeroides* ND(L166) reaction center mutant, poised in its reduced P^0 state with the addition of ascorbate, at pH 10.5, 8.0, and 5.0. The inset shows the Fourier deconvolution of the 1600−1620 cm^{-1} spectral region. Same conditions as in Figure 2.

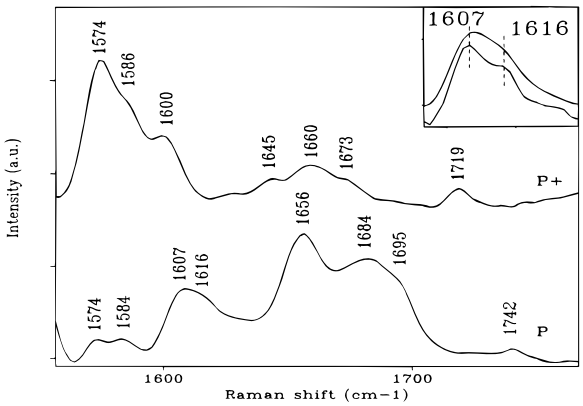

FIGURE 6: Fourier transform Raman spectra of the *Rsp. centenum* reaction center, poised in its reduced P^0 state with the addition of ascorbate and in its oxidized $P^{\bullet+}$ state with the addition of ferricyanide, both at pH 8. The inset shows the 1600−1620 cm^{-1} spectral region and its Fourier deconvolution. Same conditions as in Figure 2.

that the protonation state of the aspartate residue at L166 can be titrated. The largest difference in midpoint potential between WT and the ND(L166) mutant is observed at pH 5 to be 25 mV (Table 1).

FT Raman spectroscopy was used to monitor possible changes in the conjugated carbonyl frequencies of P in WT and the mutant RCs as a function of pH in the range of pH 5.0−10.5. For WT RCs, the P^0 FT preresonance Raman spectrum did not exhibit any measurable differences in band frequencies within 1 cm^{-1} in this pH range (data not shown). Figure 5 shows the P^0 FT Raman spectrum for the ND(L166) mutant RC resuspended in different buffers (see Materials and Methods) with pH values of 5.0, 8.0, and 10.5. The spectrum of RCs at pH 8.0 was described before (see above). The P^0 spectra of ND(L166) at pH 8.0 and 10.5 exhibit similar bands, and no shift within 1 cm^{-1} could be detected. In contrast, Fourier deconvolution of the complex band at ca. 1612 cm^{-1} indicated that, at pH 5.0, the vibrational frequency of the P_L C_2 acetyl carbonyl group downshifts by 2 cm^{-1} to 1614 cm^{-1} as compared with those corresponding frequencies observed at pH 8.0 and 10.5. For the NH(L166) mutant, there was no observable change in the FT Raman spectrum as the pH was changed from 8 to 5 (data not shown).

Near-Infrared FT (Pre)resonance Raman Spectra of Reduced and Oxidized RCs from Rsp. centenum. Figure 5 shows the near-infrared FT Raman spectra, excited using 1064 nm radiation, of the *Rsp. centenum* RCs (containing the bound tetraheme cytochrome subunit) poised in their P^0 and $P^{\bullet+}$ states, in the 1550−1800 cm^{-1} spectral region. This spectral region exhibits Raman bands arising from the C_aC_m methine bridge (ca. 1600−1610 cm^{-1}) and carbonyl group stretching modes (ca. 1620−1700 cm^{-1}). Both reduced (P^0) and oxidized ($P^{\bullet+}$) spectra were normalized with respect to the complex band at ca. 2900 cm^{-1} (arising from the C−H bonds from protein and detergent) and the carotenoid band at ca. 1520 cm^{-1} (spectral regions not shown). The P^0 spectrum is remarkably similar to that of *Rb. sphaeroides* and contains dominant contributions of P^0 over the other bacteriochlorin pigments (Mattioli *et al.*, 1991) with no interferring contributions from the cytochrome heme groups (Ivancich *et al.*, 1996b). The 1064 nm laser radiation selectively enhances the FT (pre)resonance Raman spectrum of *Rsp. centenum* RCs in their neutral (P^0) and oxidized ($P^{\bullet+}$) states via their electronic absorption maxima at 850 and 1242 nm (Wang *et al*., 1994), respectively (Mattioli *et al.*, 1991).

The broad band centered at ca.1612 cm^{-1} (23 cm^{-1} FWHM) is reminiscent of that seen in the FT Raman spectra of P in RCs of *Rvx. gelatinosus* (Agalidis *et al*., 1992) and *C. tepidum* (Ivancich *et al.*, 1996b). In Figure 6, this band can be resolved, by Fourier deconvolution and second derivative analyses, into two clear components at 1607 and 1616 cm^{-1}. Similar spectral analyses of the broad 1612 cm^{-1} band in the P^0 FT Raman spectra of *Rvx. gelatinosus* (Agalidis *et al*., 1992) and *C. tepidum* (Ivancich *et al.*, 1996b) yielded similar 1607 and 1616 cm^{-1} components. The broad band centered at ca. 1612 cm^{-1} containing components at 1607 and 1616 cm^{-1}, as well as those at 1656, 1684, and 1695 cm^{-1}, all bleach upon oxidation of P, and thus, they can be assigned to P^0 (Mattioli *et al*., 1991). New bands assignable to $P^{\bullet+}$ which appear upon oxidation of P to its $P^{\bullet+}$ state by addition of ferricyanide (Figure 3) are those at 1600, 1645, and 1719 cm^{-1} (as well as at 1574 and 1586 cm^{-1}); these bands appear (or gain in intensity) because of resonance enhancement via the 1242 nm electronic absorption band (Mattioli *et al*., 1991); these bands are assigned to $P^{\bullet+}$ of the *Rsp. centenum* RC and are similar to those in the $P^{\bullet+}$ FT Raman spectra of *Rb. sphaeroides* and *Rvx gelatinosus*, including the intensity pattern of the 1574/1586/1600 cm^{-1} cluster of bands for this latter species. The bands at 1660 and 1673 cm^{-1} cannot be unambiguously assigned to $P^{\bullet+}$. Similar bands have been observed in the $P^{\bullet+}$ FT Raman spectra of *Rb. sphaeroides* WT RCs and mutants, as well as in *Chloroflexus aurantiacus* and *C. tepidum*, and their tentative assignments have been discussed elsewhere (Mattioli *et al.*, 1991, 1994; Ivancich *et al.*, 1996a,b). The vibrational frequencies of the 1600, 1645, and 1719 cm^{-1} bands observed in the $P^{\bullet+}$ spectrum of *Rsp. centenum* are similar to those observed in that of *Rb. sphaeroides*, indicating that, in general, the extent of positive charge localization on one of the two BChls of the primary donor dimer is similar for these two RCs. Significant differences in the P^0 spectrum of *Rsp. centenum* compared to that of *Rb. sphaeroides* are seen in the vibrational frequencies of the 1616 cm^{-1} $P^{\bullet+}$ component which is 4 cm^{-1} lower in vibrational frequency with respect to its 1620 cm^{-1} counterpart in *Rb. sphaeroides* and in the 1695 cm^{-1} band which is 4 cm^{-1} higher in frequency (see Table 2). This 1616 cm^{-1} FT Raman band is similar to those observed for the NH(L166) and ND(L166) mutants at pH 8 (see above).

Table 2: Observed Frequencies and Assignments of the Methine Bridge and C_2 Acetyl Carbonyl Vibrators of Several Bacterial Primary Donors (cm^{-1})

species	P_L C_aC_m	P_M C_aC_m	P_L C_2═O	P_M C_2═O
centenum	1607	1607	1616	1656
(residue)[a]	(His L173)[e]	(His)	(His L168)	(none)
gelatinosus	1607	1607	1616	1654
(residue)[b]	(His L173)	(His M203)	(His L168)	(none)
tepidum	1607	1607	1616	1633
(residue)[c]	(His L181)	(His M201)	(His L176)	(Tyr M196)
sphaeroides	1607	1607	1620	1653
(residue)[d]	(His L173)	(His M202)	(His L168)	(none)

[a] This work. [b] Nagashima *et al.* (1993, 1994). [c] Nozawa *et al.* (1997); Ivancich *et al.* (1996b). [d] Williams *et al.* (1984). [e] Proposed axial ligand of the BChl Mg atom.

Rsp. centenum L Subunit Sequence. The nucleotide sequence of a 963-base *Bam*HI−*Xmn*I segment containing the L subunit gene was determined in both directions. The gene was identified by the similarity of the derived amino acid sequence to that of the L subunit of *Rb. sphaeroides*. The gene is 831 bases long and encodes a protein of 276 amino acid residues, including the amino-terminal methionine. Numbering of the derived amino acid sequence begins with the second residue Ala, as in *Rb. sphaeroides*. Alignment of the L subunit sequence from *Rsp. centenum* indicated 80%, 68%, 64%, and 63% identical amino acid residues with the sequences of the L subunit from *Rvx. gelatinosus*, *Rsp. rubrum*, *Rb. sphaeroides*, and *Rb. capsulatus*, respectively (Nagashima *et al.*, 1994; Bélanger *et al.*, 1988; Youvan *et al.*, 1984; Williams *et al.*, 1984). The complete sequence of the gene encoding the L subunit from *Rsp. centenum* has been submitted to the Genome Sequence Data Bank (Accession Number L81173). The gene encoding the M subunit was found to start ten nucleotides after the L subunit stop codon.

DISCUSSION

Interactions and Influence of Asn/His L166. The three-dimensional crystal structures of various strains of *Rb. sphaeroides* (Chirino *et al.*, 1994; Ermler *et al.*, 1994; Arnoux & Reiss-Husson, 1996) indicate that the carbonyl and NH_2 groups of Asn L166 are within 3.5 Å of the δ imidazole nitrogen atom of His L168 (Figure 1). Additional interactions with nearby groups are also possible for Asn L166, including H-bonds to a nearby water or with Asp M184. All of these structures indicate that Asn L166 interacts with His L168 and thus should influence the H-bond between His L168 and the primary donor. The effects of the mutations at L166 in *Rb. sphaeroides* reported in this work strongly support the existence of such interactions.

A H-bond between the NH_2 group of Asn L166 and His L168 should result in an effective strengthening of the H-bond between His L168 and the P_L acetyl carbonyl group due to an increase in net positive charge on the His L168 imidazole ring and an increase in the donating capability of the proton on its ϵ nitrogen to P_L. If there were no other changes, then one would expect to observe a strengthening of the H-bond between His L168 and P upon strengthening of the L166−L168 H-bond interaction. For the NH(L166) mutant, the H-bond between P and His L168 is stronger than that seen in WT. This stronger H-bond could be reflecting a stronger H-bond between L166 and L168. Thus the strengthening of the H-bond to the dimer in the NH(L166) mutant is consistent with the histidine residue at position L166 donating a H-bond to the δ nitrogen atom of His L168.

The ND(L166) mutation resulted in a strengthening of the H-bond between His L168 and P similar to that seen in the NH(L166) mutant. What distinguishes the ND(L166) mutant from the WT and the other mutants is that the H-bond increases in strength at low pH where Asp is expected to be protonated, with the largest shift of the 1614 cm^{-1} band evident at pH 5. This suggests that Asp L166 can be titrated and that the change in its protonation state strengthens the H-bond, probably by directly H-bonding to His L168. The shift of the 1616 cm^{-1} band at pH 8 to 1614 cm^{-1} as the pH is lowered to 5 is most likely reflecting an increase in the RC population from partially to fully protonated Asp L166.

Since the Leu side chain is incapable of donating a H-bond, the measured strengthening of the H-bond between His L168 and P upon replacement of Asn L166 with a Leu is not what would be expected for the simple removal of the proposed H-bond interaction to the δ nitrogen atom of the His L168 residue. One interpretation of this result is that Asn L166 in the native *Rb. sphaeroides* RC actually acts to effectively weaken the H-bond between His L168 and P; thus the mutation of Asn L166 would remove the interaction between Asn L166 and His L168, strengthening the H-bond between His L168 and P. For example, the asparagine carbonyl group, being electronegative, could act on the His L168 δ nitrogen atom to reduce the donation capability of the protonated ϵ nitrogen and thus weaken its H-bond with P. Alternatively, replacement of Asn L166 could result in a repositioning of His L168, resulting in a stronger H-bond with P. It is also possible that a new unidentified H-bond donor to His L168 could be present in the mutants and possibly strengthen its H-bond with P. Although this argument cannot be formally excluded, the incorporation of adventitious water seems unlikely in light of the fact that His, Leu, and Asp have comparable or larger molar volumes with respect to Asn (Zamyatnin, 1972).

In summary, the mutation of Asn L166 in *Rb. sphaeroides* results in an alteration of the H-bond strength between His L168 and the P_L C_2 acetyl carbonyl group of P as seen by the downshift of the 1620 cm^{-1} band in the WT FT Raman spectrum. Based on the relative shifts in the frequencies of this carbonyl vibrational band, the strongest bond between the primary donor and His L168 is seen in the mutant with Asp at L166 at low pH (1614 cm^{-1}), where Asp is probably predominantly protonated, then the mutants with His L168 (1616 cm^{-1}), Asp at high pH (1616 cm^{-1}), Leu (1618 cm^{-1}), and the wild type with Asn at L166 (1620 cm^{-1}). The reasons for the changes in H-bond strength appear to be complex. The data are consistent with the interpretation that His and Asp in its protonated form are proton donors in a H-bond with the δ nitrogen atom of His L168. The different strengths of the H-bond between L168 and P reflect the proton-donating ability of each residue at L166. Asn at L166 in WT could be either a weak proton donor to His L168 or predominantly interacting through the carbonyl group with His L168. Leu and Asp at high pH would not be proton donors to His L168, and the increase in the H-bond strength between His L168 and P in these situations relative to WT could be due to repositioning of His L168 or the removal of the interaction between Asn L166 and His L168.

Intensity of the 1616−1620 cm^{-1} FT Raman Band. Quantum mechanical calculations (Warshel & Parson, 1987; Parson & Warshel, 1987) indicate that the Q_y absorption band of the dimer should be sensitive to the conformation of the C_2 acetyl groups of the BChls with respect to the macrocycle planes. The blue shift of the Q_y band of the L166 mutant RCs, compared to that of wild type (Figure 2), could be reflecting a more in-planar conformation of the acetyl carbonyl group corresponding to the 1616−1620 cm^{-1} Raman band (Parson & Warshel, 1987). The FT Raman spectra of the primary donor of the L166 mutants showed that the 1620 cm^{-1} band decreased in intensity as well as shifting to lower frequencies. The relative intensity of this Raman band of P should be quite insensitive to minor changes in the preresonance condition arising from the small shifts in the dimer Q_y absorption band. A decrease in intensity of this C_2 acetyl carbonyl band would reflect either (i) a more out-of-plane conformation with the BChl macrocycle and a concomitant loss in effective π-conjugation with the macrocycle or (ii) a decrease in the polarizability of the C_2═O bond. Point i is not consistent with the above argument as there appears to be no obvious correlation between the intensity of the 1616−1620 cm^{-1} Raman band and the observed blue shift of the Q_y dimer absorption band. The decrease in intensity seems most likely to be correlated with a decrease in the polarizability of the C_2═O bond as the H-bond to this group strengthens.

pH Dependence of the P Midpoint Potential. The measured $P^0/P^{\bullet+}$ midpoint potential in isolated RCs of WT *Rb. sphaeroides* exhibits a modest pH dependence, ranging from 515 mV at pH 5 to 472 mV at pH 9.5 (Figure 4 and Table 1). Between pH 6 and 9.5, the average change in $P^0/P^{\bullet+}$ midpoint potential is about −12 mV per pH unit. During a redox titration, if the species being titrated undergoes a protonation/deprotonation as it becomes reduced/oxidized, then the midpoint potential of this species is expected to exhibit a pH dependence with the midpoint potential decreasing by −59 mV per pH unit [for example, see Cramer and Knaff (1990)]. The comparatively small pH dependence of the $P^0/P^{\bullet+}$ midpoint potential in WT *Rb. sphaeroides* RCs indicates that the primary donor, as expected, does not undergo a change in protonation state upon oxidation. If a residue near the primary donor is protonatable, then it can be expected that its protonation/deprotonation could have an influence on the midpoint potential of P via a change in its electrostatic environment resulting from the change in protonation state. This would manifest itself in a pH-dependent midpoint potential of P which should be less pronounced than −59 mV per pH unit, since it is not P itself which is changing protonation state. The modest pH dependence of the P midpoint potential that we observe here for WT is most likely due to the change in protonation state(s) of one or several amino acid residues near to, but not necessarily in the immediate vicinity of, P (Maroti & Wraight, 1988).

Charged residues near the primary donor are expected to have an electrostatic effect on its redox midpoint potential. If an altered residue in the mutant RCs can be pH titrated, and is near enough to exert an electrostatic influence on P, then the pH dependence of the $P^0/P^{\bullet+}$ midpoint redox potential of the mutant will be different than that of wild type. In the L166 series of RC mutants studied here, only the ND(L166) mutant showed a pH dependence which was significantly different from that of WT. Changing the pH from 6 to 9.5 resulted in a ca. 90 mV decrease in the midpoint potential or an average change of −25 mV per pH unit (Table 1). There was also observed a 2 cm^{-1} decrease in vibrational frequency of the Raman band assigned to the carbonyl group of P H-bonded with His L168 at pH 5, reflecting a strengthening of this H-bond as the pH is lowered from pH 8. These observations suggest that the aspartate residue at L166 is titrable and that its protonation at low pH leads to a measurable increase in the $P^0/P^{\bullet+}$ redox midpoint potential and a concomitant overall strengthening of the conserved H-bond between His L168 and the primary donor. The greatest change in $P^0/P^{\bullet+}$ midpoint potential for the ND-(L166) mutant occurs between pH 6 and 9.5, implying that the Asp residue has a pK_a somewhere in this range, significantly higher than the typical values of 4−4.8. The reason for this shift is probably due to the low dielectric environment of Asp at position L166 or perhaps due to the interaction of His L168 with the amino acid residue at position L166. Similarily, such a shift of the pK_a of the Asp residue could also have occurred for the His residue at position L166 in the NH(L166) mutant. Typically, the first pK_a value of the imidizole ring is at ca. 6, but an increase in the pK_a of the His at position L166 could explain why the $P^0/P^{\bullet+}$ midpoint potential is the same as WT for the NH-(L166) mutant in the pH range studied in this work.

Recent work on other *Rb. sphaeroides* RC mutants designed to add histidine-donated H-bonds to the conjugated carbonyl groups of P revealed a linear correlation between the number and strengths of these H-bonds (Lin *et al.* 1994a; Mattioli *et al.*, 1995). Based on this correlation, the observed strengthening in the His L168 H-bond to P would translate to a predicted 8−16 mV increase in the $P^0/P^{\bullet+}$ redox midpoint potential for the L166 mutants at pH 8. Table 1 indicates that the observed changes in the redox potentials are, in general, consistent with these predictions.

Structure of the Rsp. centenum Primary Donor. The FT Raman spectrum of P^0 in *Rsp. centenum* is very similar to those of *Rνx. gelatinosus* and *C. tepidum*, and all three are similar to those of *Rb. sphaeroides*, *Rb. capsulatus*, and *Rsp. rubrum* (Mattioli *et al*., 1992), indicating that the microenvironments of the primary donors in all these RCs are similar. This structural similarity is corroborated by the high degree of homology in the comparative sequence alignment of the L and M subunits in the region of the primary donor [see Figure 9 in Nagashima *et al*. (1994)]. The observed vibrational frequencies of the bands arising from the C_aC_m methine bridge stretching mode and the conjugated carbonyl vibrators of the *Rsp. centenum* primary donor and their assignments are given in Table 2. In the FT Raman spectrum of P^0 in *Rb. sphaeroides*, the single and narrow (14 cm^{-1} FWHM) band at ca. 1607 cm^{-1} has been assigned to the C_aC_m methine bridge stretching modes of the two BChl molecules constituting the primary donor, each BChl molecule coordinated with one axial ligand at the Mg atoms (Mattioli *et al*., 1991, 1992). The similar band observed in the P^0 FT Raman spectrum of *Rsp. centenum* reflects the same situation for this primary donor. Moreover, from the sequence alignment of the L subunits of RCs from *Rsp. centenum* RC with that of *Rb. sphaeroides* (Figure 7), *Rsp. centenum* also possesses the highly conserved His residue at position L173 of *Rb. sphaeroides*. Thus, assuming a structural homology between the structure of the *Rsp.*

Rsp. centenum	L	**H**	F	**H**	Y	N	P	A	**H**	M	I
Rvx. gelatinosus	L	**H**	F	**H**	Y	N	P	A	**H**	M	L
C. tepidum	L	**H**	F	**H**	Y	N	P	A	**H**	M	L
Rsp. rubrum	A	**N**	F	**H**	Y	N	P	A	**H**	M	L
Rb. capsulatus	G	**N**	F	**H**	Y	N	P	F	**H**	M	L
Rb. sphaeroides	G	**N**	F	**H**	Y	N	P	A	**H**	M	I
ND(L166)	G	**D**	F	**H**	Y	N	P	A	**H**	M	I
NH(L166)	G	**H**	F	**H**	Y	N	P	A	**H**	M	I
NL(L166)	G	**L**	F	**H**	Y	N	P	A	**H**	M	I
		L166		L168					L173		

FIGURE 7: Sequence alignment of the residues corresponding to L165 through L175 of the L subunit of *Rsp. centenum* and five other purple bacteria, including *Rb. sphaeroides*. Also shown are the regions for the *Rb. sphaeroides* mutants ND(L166), NH(L166), and NL(L166). *Rsp. centenum*, this work; *Rvx. gelatinosus*, Nagashima *et al.* (1994); *C. tepidum*, Nozawa *et al.* (1997) and Ivancich *et al*. (1996b); *Rsp. rubrum*, Bélanger *et al*. (1988); *Rb. capsulatus*, Youvan *et al.*, (1984); *Rb. sphaeroides*, Williams *et al*. (1984).

centenum RC and that of *Rb. sphaeroides*, we may propose that the sole axial ligands of P_L and P_M are histidines, including L173 (see Table 2).

The 1616 cm^{-1} component (Figure 6 and inset) resembles the 1620 cm^{-1} band of the P_L acetyl carbonyl in the FT Raman spectra of other purple primary donors (Mattioli *et al*., 1992); because of their low frequency, these bands can only be assigned to a H-bonded C_2 acetyl carbonyl group (Mattioli *et al.*, 1991), and for the case of *Rb. sphaeroides*, the 1620 cm^{-1} band was assigned to the P_L C_2 acetyl carbonyl which is H-bonded to His L168 (Mattioli *et al.*, 1991, 1994). Similar 1616 cm^{-1} components were also observed in the P^0 FT Raman spectra of *Rvx. gelatinosus* (Agalidis *et al*., 1992) and *C. tepidum* (Ivancich *et al.*, 1996b); in both cases the 1616 cm^{-1} bands were assigned to a H-bonded acetyl carbonyl group, the analogous P_L C_2 acetyl carbonyl group of P of *Rb. sphaeroides*. The recently published primary structure for the analogous L and M subunits of *Rvx. gelatinosus* (Nagashima *et al*., 1993, 1994) and those of *C. tepidum* (Nozawa *et al.*, 1997; Ivancich *et al.*, 1996b) showed that both these species possess a His residue at the equivalent position of His L168 in *Rb. sphaeroides* as was suggested previously on the basis of the similarities of the FT Raman spectra of the two RCs (Agalidis *et al.*, 1992; Ivancich *et al.*, 1996b). In all these species the H-bond donor to the C_2 acetyl carbonyl of P_L is a His residue, but for *Rvx. gelatinosus*, *C. tepidum*, and *Rsp. centenum* the observed vibrational frequency for this acetyl group is significantly lower than the other species [4−8 cm^{-1}; compare Table 2 in Mattioli *et al*. (1992) and Figure 6].

Other observed bands in the P^0 spectrum of Figure 6 corresponding to the other conjugated carbonyl groups of P can also be assigned. The 1683 and 1696 cm^{-1} bands are only consistent with C_9 keto carbonyl groups not engaged in H-bond interactions with the protein (Lutz, 1984; Mattioli *et al*., 1991). The 1654 cm^{-1} band is assigned to the P_M C_2 acetyl carbonyl group that is free from interactions as it was for the primary donors of *Rb. sphaeroides* (Mattioli *et al*., 1994), *Rvx. gelatinosus* (Agalidis *et al*., 1992), and other purple bacterial species (Mattioli *et al*., 1992). The vibrational frequency for the P_L C_9 keto carbonyl (1696 cm^{-1}) appears to be 5 cm^{-1} higher than that of the equivalent conjugated carbonyl in *Rb. sphaeroides* (1691 cm^{-1}; Mattioli *et al*., 1991, 1994).

As mentioned before, the bands at 1600, 1645, and 1719 cm^{-1} in Figure 6 arise from $P^{\bullet+}$. These bands are very similar to those seen in the $P^{\bullet+}$ FT Raman spectra of *Rvx. gelatinosus* (Agalidis *et al*., 1992), *C. tepidum* (Ivancich *et al.*, 1996b), and *Rb. sphaeroides* (Mattioli *et al*., 1991, 1994). In the FT Raman spectrum of *Rb. sphaeroides* oxidized RCs, bands were observed at 1600, 1641, and 1717 cm^{-1}; they were assigned to the C_aC_m methine stretching mode (downshifted from 1607 cm^{-1} upon P oxidation) and to C_2 acetyl and C_9 keto carbonyl groups of P_L upshifted from 1620 and 1691 cm^{-1}, respectively, upon P oxidation; these assignments were made on the basis of the expected behavior of the vibrational frequencies of the C_aC_m (downshifting) and the π-conjugated carbonyl (upshifting) upon the oxidation of a BChl species with a HOMO of a_{1u} orbital symmetry [(discussed in Mattioli *et al*. (1991, 1994)]. For the *Rsp. centenum* $P^{\bullet+}$ spectrum, the 1600 cm^{-1} band is consistent with a C_aC_m stretching mode which has downshifted by 7 cm^{-1} (1607 cm^{-1} in P^0, Figure 6) upon P oxidation. Considering similar resonance conditions for *Rb. sphaeroides* and *Rsp. centenum* P spectra in the cation radical state, the bands at 1645 and 1719 cm^{-1} arise from the P_L C_2 cetyl and C_9 keto carbonyl groups, respectively. The other observed bands in the spectrum of Figure 6 at 1660 and 1673 cm^{-1} cannot be unambiguously assigned to $P^{\bullet+}$ since they may have been masked by the stronger carbonyl bands in the P^0 spectrum (Figure 6); similar bands in the $P^{\bullet+}$ spectrum of *Rb. sphaeroides* were ascribed to (i) (1659 cm^{-1}) BChl *a* molecules (other than the primary donor) or protein contributions (Mattioli *et al*., 1991; Beekman *et al*., 1995) and (ii) (1680 cm^{-1}) BPhe molecule contributions (Ivancich *et al*., 1996a).

Resonance Raman spectroscopy is a useful technique in analyzing the extent of charge distribution in porphyrin radical complexes (Bradley *et al.*, 1981; Donohoe & Bocian 1990; Tran-Thi *et al.*, 1994). As previously discussed, the upshift of the P_L C_9 keto carbonyl band in the FT Raman spectrum of *Rb. sphaeroides* RCs upon oxidation can be used to estimate the degree of positive charge localization on the P_L constituent of the primary donor (Mattioli *et al.*, 1991, 1992, 1994, 1995). The observed upshift of the 1695 cm^{-1} band arising from the C_9 keto carbonyl of P_L in the reduced P^0 *Rsp. centenum* FT Raman spectrum to 1719 cm^{-1} indicates that ca. 75% of the resulting + charge is on the P_L constituent; this situation is similar to the 72−80% found for *Rb. sphaeroides* [see Mattioli *et al.* (1991, 1994)].

In summary, the primary donor structure and protein H-bond interactions of *Rsp. centenum* appear to be quite similar to those of *Rb. sphaeroides*, where the only H-bond observed is one between the P_L C_2 acetyl carbonyl and the conserved histidine residue at position L168 of *Rb. sphaeroides* (Table 1). This H-bond appears to be stronger for the case of *Rsp. centenum* than for *Rb. sphaeroides*. The analogous H-bond to a C_2 acetyl carbonyl group of P observed for the primary donor of *Rvx. gelatinosus* (Agalidis *et al.*, 1992), and of *C. tepidum* (Ivancich *et al.*, 1996b), is also stronger than that of *Rb. sphaeroides* and similar in strength to that of *Rsp. centenum*. Comparing the partial sequence alignments of the L subunit from *Rsp. centenum*, *Rb. sphaeroides*, *Rsp. rubrum*, and *Rb. capsulatus* near the primary donor and in particular near L168, the most significant difference appears to be at L166 (Figure 7). For *Rb. sphaeroides*, *Rb. capsulatus*, and *Rsp. rubrum*, an

asparagine residue is found at position L166; however, for *Rsp. centenum* a histidine residue is found at L166 as is the case for *Rvx. gelatinosus* (Nagashima *et al.*, 1994) as well as *C. tepidum* (Nozawa *et al.*, 1997; Ivancich *et al*., 1996b).

Comparison of the Primary Donors of NH(L166) Rb. sphaeroides Mutant and Rsp. centenum. As mentioned above, the observed 1616 cm^{-1} band in the P^0 FT Raman spectra of *Rsp. centenum* RCs (Figure 6), as well as those of *Rvx. gelatinosus* (Agalidis *et al*., 1992) and *C. tepidum* (Ivancich *et al*., 1996b), is assigned to the P_L C_2 acetyl carbonyl group, H-bonded to a His residue at equivalent position of His L168 in *Rb. sphaeroides*. The NH(L166) *Rb. sphaeroides* mutant, which was designed to mimic the FT Raman spectrum of *Rsp. centenum*, as well as those of *Rvx. gelatinosus* and *C. tepidum*, exhibits the downshift of the 1620 cm^{-1} band to 1616 cm^{-1}. This 4 cm^{-1} downshift relative to *Rb. sphaeroides* and other species where position L166 is occupied by an asparagine residue seems to result from an interaction of His L166 (present in the latter species) with His L168, thus strengthening its H-bond with the C_2 acetyl of P_L.

Based on a previous study which correlated the $P^0/P^{\bullet+}$ redox midpoint potential of *Rb. sphaeroides* RC mutants and H-bond interaction, the increase in the H-bond strength reflected by the decrease in vibrational frequency of 4 cm^{-1} is expected to only modestly raise the midpoint potential by ca. 10 mV (Mattioli *et al.*, 1995). As well, the measured $P^0/P^{\bullet+}$ redox midpoint potential of the NH(L166) mutant at pH 8 was observed to be ca. +30 mV higher relative to that of WT. Thus, it can be expected that the $P^0/P^{\bullet+}$ redox midpoint potential of *Rsp. centenum* should be approximately the same or more positive than that of *Rb. sphaeroides*. However, the $P^0/P^{\bullet+}$ redox midpoint potential in isolated RCs of *Rsp. centenum* at pH 8, possessing the RC-associated tetraheme cytochrome, is about 25 mV lower than that of *Rb. sphaeroides* (Wang *et al.*, 1994), indicating that other factors influence its effective redox potential. Recently, we have reported the influence of the RC-associated tetraheme cytochrome on the absorption, redox, and FT Raman spectral properties of the *C. tepidum* RC (Ivancich *et al.*, 1996b). These studies showed that the presence of the tetraheme cytochrome resulted in a ca. 10 nm red shift of the P absorption band and a ca. 30 mV decrease in the $P^0/P^{\bullet+}$ midpoint potential; there were no measureable changes in the FT Raman spectrum of P, and thus it was concluded that the influence of the tetraheme cytochome was of an electrostatic nature and not due to sizable conformational changes in the P microenvironment. The presence of the tetraheme cytochrome in the *Rsp. centenum* RC preparations studied here probably partially accounts for the lower $P^0/P^{\bullet+}$ midpoint potential compared to *Rb. sphaeroides* and may be masking the intrinsic effect of the histidine residue at position L166.

It is clear that effects of an asparagine or histidine residue at position L166 are not major and do not modulate the redox properties of P to the same extent as do residues such as His L168 which are directly interacting with P. However, the interaction between Asn/His L166 and His L168 that we propose in this paper may have a role in slightly fine tuning the redox properties of the primary donor in purple bacteria and thus optimizing the redox compatibilites between the RC-associated cytochrome, P, and the primary quinone acceptor. It is interesting to note that species of purple bacteria which possess histidine at the homologous position L166 of *Rb. sphaeroides* are those which have RC-associated tetraheme cytochromes (Nagashima *et al.*, 1993, 1994; Nitschke & Dracheva, 1995; Nozawa *et al.*, 1997; Ivancich *et al.*, 1996). Species which have no RC-associated tetraheme cytochrome but rather a monoheme cytochrome, such as *Rb. sphaeroides*, *Rb. capsulatus*, and *Rsp. rubrum*, have asparagine at position L166 (Komiya *et al.* 1988). The only known exceptions are *Cf. aurantiacus* and *Rps. viridis* which both have RC-associated tetraheme cytochromes but asparagine is found at position L166. The X-ray crystal structure of the *Rps. viridis* RC (Deisenhofer & Michel, 1989; Deisenhofer *et al.*, 1995) indicates that the NH_2 group of Asn L166, as compared to that of *Rb. sphaeroides*, is slightly further away from the δ imidazole nitrogen atom of His L168 (4.18 Å) and thus probably not forming a H-bond directly to His L168. However, the structure indicates that a water molecule is present between the NH_2 group of Asn L166 and the δ imidazole nitrogen atom of His L168 and is in a position to make a H-bond bridge between these two residues. Furthermore, there is another water molecule which may form another H-bond with the NH_2 group of Asn L166 in a similar position as that for *Rb. sphaeroides* (see Figure 1); there is still another water molecule which is near enough to the carbonyl group of Asn L166 to form a further H-bond with this residue at its carbonyl group. No such information is available for the *Cf. aurantiacus* RC.

CONCLUSIONS

In the reaction center of *Rb. sphaeroides*, Asn L166 is in interaction with His L168 which is H-bonded to the C_2 acetyl carbonyl of P_L. Replacement of Asn L166 in these reaction centers with a histidine residue increases the strength of the H-bond between His L168 and P_L. The strength of this H-bond is similar to what is observed in the FT Raman spectra of native reaction centers of other photosynthetic bacteria where a histidine residue at the analogous L166 position is naturally found, e.g., *Rsp. centenum*, *Rvx. gelatinosus*, and *C. tepidum*; these latter species all possess a reaction center-associated tetraheme cytochrome. Mutations at the L166 position in *Rb. sphaeroides* are seen to alter the $P^0/P^{\bullet+}$ midpoint potential by as much as 55 mV. Interactions between His L168, which is strongly conserved in purple bacteria, and the residue at position L166 may serve as a mechanism to fine tune the $P^0/P^{\bullet+}$ midpoint potential with that of the tetraheme cytochrome. The hydrogen-bonding network formed by these residues would also serve as a favorable pathway for electron transfer (Beraton *et al.*, 1991) from the cytochrome heme to P.

ACKNOWLEDGMENT

We thank Drs. Françoise Reiss-Husson, Ileana Agalidis, and Alain Desbois for helpful discussions. We also thank Xuan Nguyen for assistance with mutagenesis and isolation of the reaction centers and Carl Bauer for providing the *Rsp. centenum* cosmid.

REFERENCES

Agalidis, I., Robert, B., Mattioli, T. A., & Reiss-Husson, F. (1992) in *The Photosynthetic Bacterial Reaction Center II: Structure, Spectroscopy, and Dynamics* (Breton, J., & Vermeglio, A., Eds.) pp 133−139, Plenum, New York.

Allen, J. P., & Williams, J. C. (1995) *J. Bioenerg. Biomembr. 27*, 275−283.

Allen, J. P., Feher, G., Yeates, T. O., Komiya, H., & Rees, D. C. (1987) *Proc. Natl. Acad. Sci. U.S.A. 84*, 5730−5734.
Arnoux, B., & Reiss-Husson, F. (1996) *Eur. Biophys. J. 24*, 233−242.
Barik, S. (1993) in *PCR Protocols: Current Methods and Applications* (White, B. A., Ed.) pp 277−286, Humana Press, Totowa, NJ.
Beekman, L. M. P., Visschers, R., Monhouwer, R., Heer-Dawson, M., Mattioli, T. A., McGlynn, P., Hunter, C. N., Robert, B., van Stokkum, I. H. M., van Grondelle, R., & Jones, M. R. (1995) *Biochemistry 34*, 14712−12721.
Bélanger, G., Bérard, J., Corriveau, P., & Gingras, G. (1988) *J. Biol. Chem. 263*, 7632−7638.
Beraton, D. N., Betts, J. N., & Onuchic, J. N. (1991) *Science 252*, 1285−1288.
Bradley, P. G., Kress, N., Hornberger, B. A., Dallinger, R. F., & Woodruff, W. H. (1981) *J. Am. Chem. Soc. 103*, 7441−7446.
Chirino, A. J., Lous, E. J., Huber, M., Allen, J. P., Schenck, C. C., Paddock, M. L., Feher, G., & Rees, D. C. (1994) *Biochemistry 33*, 4584−4593.
Cramer, W. A., & Knaff, D. B. (1990) *Energy Transduction in Biological Membranes*, pp 43−45, Springer-Verlag, New York.
Deisenhofer, J., & Michel, H. (1989) *EMBO J. 8*, 47−54.
Deisenhofer, J., Epp, O., Sinning, I., & Michel, H. (1995) *J. Mol. Biol. 246*, 429−457.
Donohoe, R. J., & Bocian, D. F. (1990) *J. Am. Chem. Soc. 112*, 8807−8811.
El-Kabbani, O., Chang, C.-H., Tiede, D., Norris, J., & Schiffer, M. (1991) *Biochemistry 30*, 5361−5369.
Ermler, U., Fritzsch, G., Buchanan, S. K., & Michel, H. (1994) *Structure 10*, 925−936.
Imhoff, J. F. (1995) in *Anoxygenic Photosynthetic Bacteria* (Blankenship, R. E., Madigan, M. T., & Bauer, C. E., Eds.) pp 1−15, Kluwer, The Netherlands.
Ivancich, A., Feick, R., Ertlmaier, A., & Mattioli, T. A. (1996a) *Biochemistry 35*, 6126−6135.
Ivancich, A., Kobayashi, M., Drepper, F., Fathir, I., Saito, T., Nozawa, T., & Mattioli, T. A. (1996b) *Biochemistry 35*, 10529−10538.
Kawaski, H., Hoshino, Y., Kuraishi, H., & Yamasoto, K. (1992) *J. Gen. Appl. Microbiol. 38*, 541−551.
Komiya, H., Yeates, T. O., Rees, D. C., Allen, J. P., & Feher, G. (1988) *Proc. Natl. Acad. Sci. U.S.A. 85*, 9012−9016.
Lin, X., Murchison, H. A., Nagarajan, V., Parson, W. W., Allen, J. P., & Williams, J. C. (1994a) *Proc. Natl. Acad. Sci. U.S.A. 91*, 10265−10269.
Lin, X., Williams, J. C., Allen, J. P., & Mathis, P. (1994b) *Biochemsitry 33*, 13517−13523.
Lutz, M. (1984) in *Advances in Infrared and Raman Spectroscopy* (Clarck, R. J. H., & Hester, R. E., Eds.) Vol. 11, pp 211−300, Wiley, New York.
Maroti, P., & Wraight, C. A. (1988) *Biochim. Biophys. Acta 934*, 329−347.
Mattioli, T. A., Hoffmann, A., Robert, B., Schrader, B., & Lutz, M. (1991) *Biochemistry 30*, 4648−4654.
Mattioli, T. A., Robert, B., & Lutz, M. (1992) in *The Photosynthetic Bacterial Reaction Center II: Structure, Spectroscopy, and Dynamics* (Breton, J., & Vermeglio, A., Eds.) pp 127−132, Plenum Press, New York.
Mattioli, T. A., Williams, J. C., Allen, J. P., & Robert, B. (1994) *Biochemistry 33*, 1636−1643.
Mattioli, T. A., Lin, X., Allen, J. P., & Williams, J. C. (1995) *Biochemistry 34*, 6142−6152.
Michel, H., Epp, O., & Deisenhofer, J. (1986) *EMBO J. 5*, 2445−2451.
Nagashima, K. V. P., Shimada, K., & Matsuura, K. (1993) *Photosynth. Res. 36*, 185−191.
Nagashima, K. V. P., Matsuura, K., Ohyama, S., & Shimada, K. (1994) *J. Biol. Chem. 269*, 2477−2484.
Nitschke, W., & Dracheva, S. (1995) in *Anoxygenic Photosynthetic Bacteria* (Blankenship, R. E., Madigan, M. T., & Bauer, C. E., Eds.) pp 775−805, Kluwer, The Netherlands.
Nozawa, T., Trost, J. T., Fukada, T., Hatano, M., McManus, J. D., & Blankenship, R. E. (1987) *Biochim. Biophys. Acta 894*, 468−476.
Nozawa, T., Fathir, N., Yoza, K., Kojima, A., Tanaka, K., Kobayashi, M., Wang, Z.-Y., & Lottspeich, F. (1997) *Photosynth. Res.* (in press).
Paddock, M. L., Rongey, S. H., Feher, G., & Okamura, M. Y. (1989) *Proc. Natl. Acad. Sci. U.S.A. 86*, 6602−6606.
Parson, W. W., & Warshel, A. (1987) *J. Am. Chem. Soc. 109*, 6152−6163.
Romijn, J. C., & Amesz, J. (1977) *Biochim. Biophys. Acta 461*, 327−338.
Sanger, F., Nicklen, S., & Coulson, A. R. (1977) *Proc. Natl. Acad. Sci. U.S.A. 74*, 5463−5467.
Tran-Thi, T.-H., Mattioli, T. A., Chabach, D., de Cian A., & Weiss, R. (1994) *J. Phys. Chem. 98*, 8279−8288.
Wang, S., Lin, S., Lin, X., Woodbury, N. W., & Allen, J. P. (1994) *Photosynth. Res. 42*, 203−215.
Warshel, A., & Parson, W. W. (1987) *J. Am. Chem. Soc. 109*, 6143−6152.
Weckesser, J., Mayer, H., & Schulz, G. (1995) in *Anoxygenic Photosynthetic Bacteria* (Blankenship, R. E., Madigan, M. T., & Bauer, C. E., Eds.) pp 207−230, Kluwer, The Netherlands.
Williams, J. C., Steiner, L. A., Feher, G., & Simon, M. I. (1984) *Proc. Natl. Acad. Sci. U.S.A. 81*, 7303−7307.
Williams, J. C., Alden, R. G., Murchison, H. A., Peloquin, J. M., Woodbury, N. W., & Allen, J. P. (1992) *Biochemistry 31*, 11029−11037.
Woese, C. R. (1987) *Microbiol. Rev. 51*, 221−271.
Yanisch-Perron, C. Vieira, J., & Messing, J. (1985) *Gene 33*, 103−119.
Yeates, T. O., Komiya, H., Chirino, A., Rees, D. C., & Feher, G. (1988) *Proc. Natl. Acad. Sci. U.S.A. 85*, 7993−7997.
Yildiz, F. H., Gest, H., & Bauer, C. E. (1992a) in *Research in Photosynthesis* (Murata, N., Ed.) Vol. III, pp 19−26, Kluwer, The Netherlands.
Yildiz, F. H., Gest, H., & Bauer, C. E. (1992b) *Mol. Microbiol. 6*, 2683−2691.
Youvan, D. C., Bylina, E. J., Alberti, M., Begusch, H., & Hearst, J. E. (1984) *Cell 37*, 949−957.
Zamyatnin, A. A. (1972) *Prog. Biophys. Mol. Biol. 24*, 107−123.

BI962516U